Molecular Therapy
Nucleic Acids
Original Article

Cross-Species Suppression of Hepatoma Cell Growth and Migration by a *Schistosoma japonicum* MicroRNA

Yu Lin,[1,3] Shanli Zhu,[1,3] Chao Hu,[1] Jing Wang,[1] Pengyue Jiang,[1] Liufang Zhu,[1] Zhengli Li,[1] Sai Wang,[1] Yuanbin Zhang,[1] Xindong Xu,[1] and Weiqing Pan[1,2]

[1]Institute for Infectious Diseases and Vaccine Development, Tongji University School of Medicine, Shanghai, China; [2]Department of Tropical Diseases, Second Military Medical University, Shanghai, China

***Schistosoma japonicum* eggs trapped in host liver secretes microRNA (miRNA)-containing extracellular vesicles (EVs) that can be transferred to host cells. Recent studies demonstrated that miRNAs derived from plants can modulate gene expression and phenotype of mammalian cells in a cross-kingdom manner. In this study, we identified a *Schistosoma japonicum* miRNA (e.g., Sja-miR-3096) that is present in the hepatocytes of mice infected with the parasite and has notable antitumor effects in both *in vitro* and *in vivo* models. The Sja-miR-3096 mimics suppressed cell proliferation and migration of both murine and human hepatoma cell lines by targeting phosphoinositide 3-kinase class II alpha (*PIK3C2A*). We generated a murine hepatoma cell line that stably expressed the pri-Sja-miR-3096 gene and demonstrated cross-species processing of the schistosome pri-miRNA to the mature Sja-miR-3096 in the mammalian cell. Importantly, inoculation of this cell line into the scapula and livers of mice led to a complete suppression of tumorigenesis of the hepatoma cells. Moreover, tumor weight was significantly reduced on intravenous administration of Sja-miR-3096 mimics. Thus, the schistosome miRNA-mediated antitumor activity occurs in host liver cells during schistosome infection, which may strengthen resistance of host to liver cancer, and discovery and development of such miRNAs may present promising interventions for cancer therapy.**

INTRODUCTION

MicroRNAs (miRNAs) are a class of highly conserved, small noncoding RNAs that regulate gene expression posttranscriptionally through binding to their target mRNAs.[1] miRNAs extensively impact progression of many human diseases such as cancers.[2,3] Dysregulations of some miRNA expression promote the occurrence and development of diverse cancers,[4,5] while others exert antitumor effects on many cancers through regulation of tumor-related genes.[6,7] Recent studies indicated that miRNAs can be delivered to other cells through extracellular vesicles (EVs) to modulate the gene expression and phenotype of distant recipient cells.[8] Strikingly, some plant-derived miRNAs can modulate expression of their target genes in mammals in a cross-kingdom manner.[9–11] For example, miR-168a derived from the food plant *Oryza sativa* modulates plasma low-density lipoprotein (LDL) levels by targeting LDL receptor adaptor protein 1 of mice,[10] while the plant miR-159 that was detectable in human sera inhibited breast cancer growth by targeting the *TCF7* gene.[9] These data indicate that heterogeneous miRNAs from food plants could be translocated into blood and modulate cell functions in mammals. However, it is not clear how these plant miRNAs can survive the passage through the gastrointestinal tract following digestion.

Several studies also revealed that the miRNAs mediated communication between the host and pathogen. *Heligmosomoides polygyrus*, a nematode parasite, secretes the miRNAs-containing exosome. Administration of the parasite exosomes to mice suppressed type 2 innate responses and eosinophilia likely through regulation of mouse genes involved in inflammation and immunity.[12] Stern-Ginossar et al.[13] reported that a human cytomegalovirus miRNA, hcmv-miR-UL112, regulates the major histocompatibility complex class I–related chain B (*MICB*) gene during viral infection and affects NK cell killing. In addition, bacteria could utilize endogenous RNAs to affect *Caenorhabditis elegans* physiology.[14] These data revealed that miRNAs-mediated cross-species interactions exist between the pathogen and host.

S. japonicum is the causative agent of intestinal schistosomiasis. Adult schistosome worm pairs live in the mesenteric veins of hosts where they lay numerous eggs, many of which are trapped in the liver tissues via the portal venous system. The live miracidia in mature eggs secrete toxins that induce granulomatous reaction and hepatic fibrosis in the host. In the granuloma, the parasite eggs are surrounded by host cells, including immunocytes, other hepatic mesenchymal cells, and hepatocytes. Our previous studies revealed that *S. japonicum* secretes a large number of miRNAs, including

Received 28 December 2018; accepted 8 September 2019;
https://doi.org/10.1016/j.omtn.2019.09.006.

[3]These authors contributed equally to this work.

Correspondence: Weiqing Pan, PhD, Institute for Infectious Diseases and Vaccine Development, Tongji University School of Medicine, Shanghai 200092, China.
E-mail: wqpan0912@aliyun.com

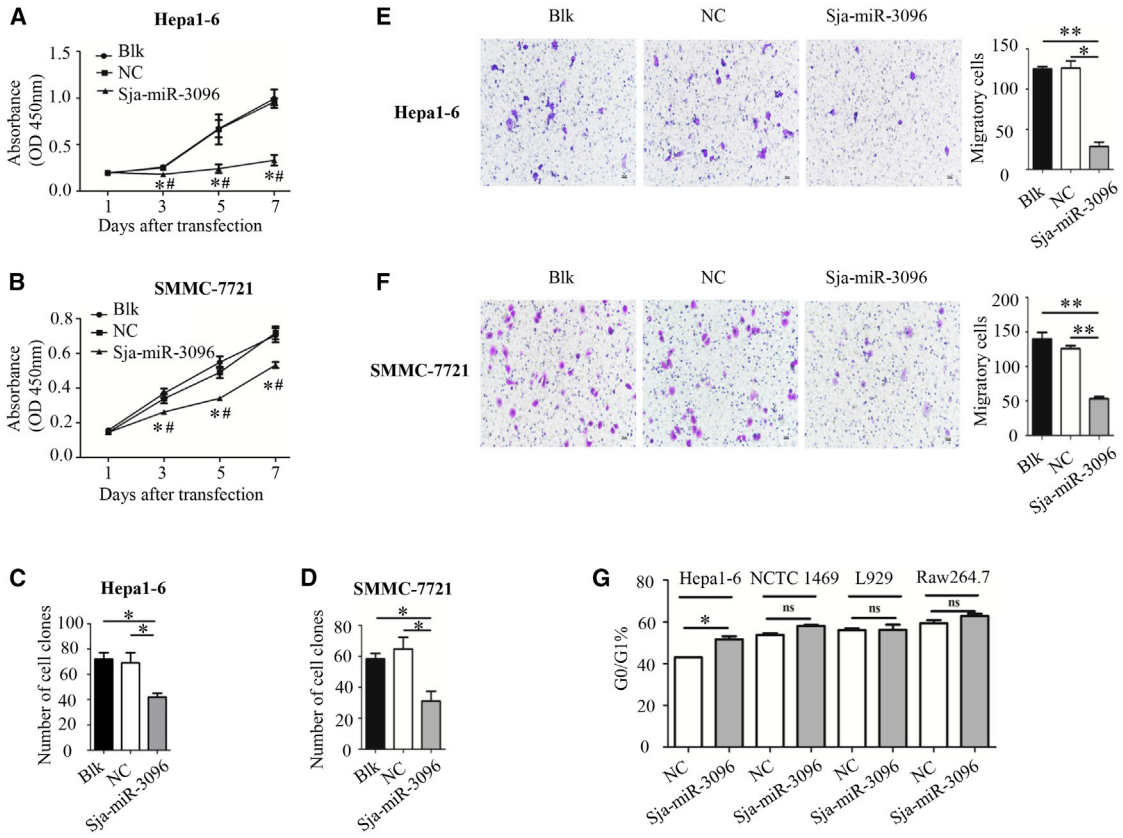

Figure 1. Inhibition of *In Vitro* Proliferation and Migration of Hepatoma Cell Lines by Sja-miR-3096

The murine hepatoma Hepa1-6 cell line (A, C, and E) and human hepatoma cell line SMMC-7721 (B, D, and F) were transfected with either Sja-miR-3096 or NC mimics and then subjected to proliferation analysis by CCK-8 assay (A and B) and colony formation (C and D) and cell migration analysis by a transwell migration assay (E and F). $^{\#}p < 0.05$ compared to Blk; $^{*}p < 0.05$ compared to NC (A and B). (G) The Hepa1-6 cell line, non-tumor cell lines of the NCTC liver cell 1469, fibroblast cell L929, and macrophage cell Raw264.7 were transfected with Sja-miR-3096 or NC mimics, and then the cell cycle was analyzed by flow cytometry. NC, a negative control mimic that has no target gene; Blk, transfection reagents only. Data are presented as mean ± SEM of three independent experiments ($^{*}p < 0.05$, $^{**}p < 0.01$; ns, no significant difference). See also Figures S2 and S3.

conserved and *Schistosoma*-specific miRNAs.[15,16] Recent studies indicated that the eggs trapped in liver also secrete parasite miRNA-containing EVs such as exosomes.[17] Unlike the plant miRNAs that need to pass through the gastrointestinal tract, the schistosome miRNAs from eggs trapped in liver tissue could directly be transferred to the neighboring host cells via EVs.[17] Therefore, we hypothesized that some parasite miRNAs from the eggs in host liver could be translocated into neighboring hepatocytes to exert various biological effects. We also speculated that some of these intake miRNAs may exert the effects that are beneficial to the host, for example, strengthening resistance of host-to-host diseases such as cancers, as the plant-derived miRNAs suppressed cancer cell growth.[9] To investigate this hypothesis, we performed genome-wide screening of miRNAs of *S. japonicum* (Sja-miRNAs) for their anti-tumor activities and detection of their presence in host liver cells. We showed that a schistosome miRNA (Sja-miR-3096) that is present in hepatocytes during schistosome infection highly inhibited the growth of tumor cells through both *in vitro* and *in vivo* models by cross-species regulation of the phosphoinositide 3-kinase class II alpha (*PIK3C2A*) gene. In addition, we reveal the cross-species processing of the schistosome pri-miRNA to the mature miR-3096 in mammalian cells.

RESULTS

Screening and Identification of Sja-miRNAs That Suppress Tumor Cell Viability

To identify schistosome miRNAs that may be involved in the suppression of tumor cell growth, we synthesized 74 Sja-miRNA mimics that were identified by us and other groups.[15,16,18,19] These miRNAs were classified into conserved miRNAs (total of 11 miRNAs) and schistosome-specific miRNAs (total of 63 miRNAs) based on their seed sequence. The synthesized mimics of the Sja-miRNAs were transfected into the Hepa1-6 hepatoma cells. Cell viability and cell cycle of the transfected cells were evaluated by Cell Counting Kit-8 (CCK-8) assay and FACS, respectively. Based on the initial screening, we found three Sja-miRNAs, i.e., Sja-miR-7, Sja-miR-124,

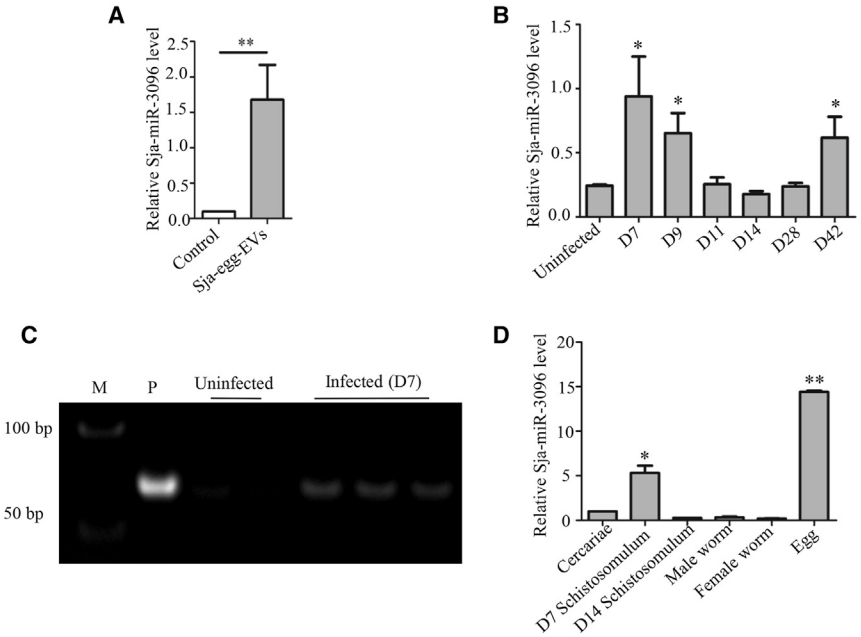

Figure 2. Detection of Sja-miR-3096 in Host Hepatocytes and Schistosome EVs

(A) Stem-loop qRT-PCR was used to validate the presence of Sja-miR-3096 in *S. japonicum* egg-derived EVs (control: wash buffer from the EV extraction process) and host hepatocytes (B) during schistosome infection. Data are presented as the mean ± SEM values (n = 3). **p < 0.01 versus the control group (A), *p < 0.05 versus uninfected group (B). (C) PCR product of Sja-miR-3096 (65 bp) in host hepatocytes and the results of 12% PAGE: lane 1, marker; lane 2, positive control; lanes 3 and 4, uninfected hepatocytes; lanes 5–7, three infected hepatocyte samples at postinfection day 7. (D) Stem-loop qRT-PCR was used to detect the relative expression of Sja-miR-3096 in five different life stages of *S. japonicum*. Data are presented as mean ± SEM of three independent experiments. *p < 0.05 versus cercariae; **p < 0.01 versus cercariae (D). See also Figures S4 and S5.

and Sja-miR-3096, that significantly suppressed cell viability (Figures S1A–S1D). Furthermore, FACS analysis revealed that the cell cycle was arrested at the G_0/G_1 phase in the hepatoma cells transfected with the three Sja-miRNAs (Figures S1E and S1F). Of the three miRNAs, Sja-miR-3096 is a schistosome-specific miRNA that showed a stronger inhibitory effect on the cell cycle compared with the others. Thus, this miRNA was selected for further evaluation of its antitumor activity and mechanism underpinning the effect.

Effects of Sja-miR-3096 on Proliferation and Migration of Tumor and Non-tumor Cells *In Vitro*

To investigate the antitumor effects of Sja-miR-3096, we transfected its mimics into the murine hepatoma Hepa1-6 cells or human hepatoma SMMC-7721 cells.[20,21] As shown in Figures 1A–1D, Sja-miR-3096 significantly inhibited *in vitro* cell proliferation and colony formation of both cell lines compared with the negative control (NC; a control mimic that has no target gene in mice) and blank control (Blk; transfection reagents only). Moreover, this schistosome miRNA also significantly inhibited the migration of the hepatoma cell lines, as shown by the results of both a transwell migration assay (Figures 1E and 1F) and a wound healing assay (Figure S2).

To evaluate whether Sja-miR-3096 affects the growth of non-tumor cell lines, we transfected the similar amount of the miRNA mimics into several non-tumor cell lines, including the liver cell line NCTC clone 1469, murine fibrosarcoma cell line L929, and murine macrophage cell line Raw264.7 (Figure S3). As shown in Figure 1G, Sja-miR-3096 has no effect on cell cycle of these non-tumor cell lines, implying that the schistosome miRNA may have no visible effect on the normal cell lines.

Cross-Species Transfer of Sja-miR-3096

We next investigated whether Sja-miR-3096 is present in the infected host liver cells or schistosome EVs that may mediate transportation of the miRNA into host cells.[17] We showed that Sja-miR-3096 was detected in the EVs isolated from schistosome eggs (Figures S4A–S4C; Figure 2A); its presence was confirmed through cloning and sequencing of the PCR product. To detect the miRNA in the infected liver cell, we prepared and carefully analyzed RNA samples of infected liver cells to ensure no contamination with parasite RNA in the infected samples (Figure S5A). We showed that Sja-miR-3096 was detected in the hepatocytes from infected mice in the early stage (i.e., day 7 and 9 postinfection) and late stage of infection (day 42) (Figure 2B), although the abundance of the parasite miRNAs was lower than that of mammalian endogenous miRNAs in the hepatocytes (Figure S5B). The presence of Sja-miR-3096 in the samples at day 7 postinfection was further verified by PAGE (Figure 2C). Furthermore, the sequence of the PCR product of Sja-miR-3096 is identical to its reference sequence by cloning and sequencing (Figure S5C). In accordance with this result, high expression of this miRNA was observed in the early-stage parasite (i.e., day 7 schistosomulum) and eggs (Figure 2D), which was consistent with previous findings by another group.[22] These findings indicate that this miRNA is present in the infected liver cells.

Inhibitory Effect of Sja-miR-3096 on Hepatoma Cell Growth *In Vivo*

To investigate whether Sja-miR-3096 inhibits *in vivo* growth of the hepatoma cells, both Hepa1-6 and SMMC-7721 cells transfected with Sja-miR-3096 mimics or the NC miRNA mimics were injected subcutaneously (s.c.) to generate subcutaneous tumors in nude mice. As shown in Figures 3A–3C, both tumor volumes and weights were significantly reduced in the mice inoculated with Hepa1-6 cells transfected with Sja-miR-3096 mimics compared to those with NC. Moreover, we showed that Sja-miR-3096 was detectable in the tumors

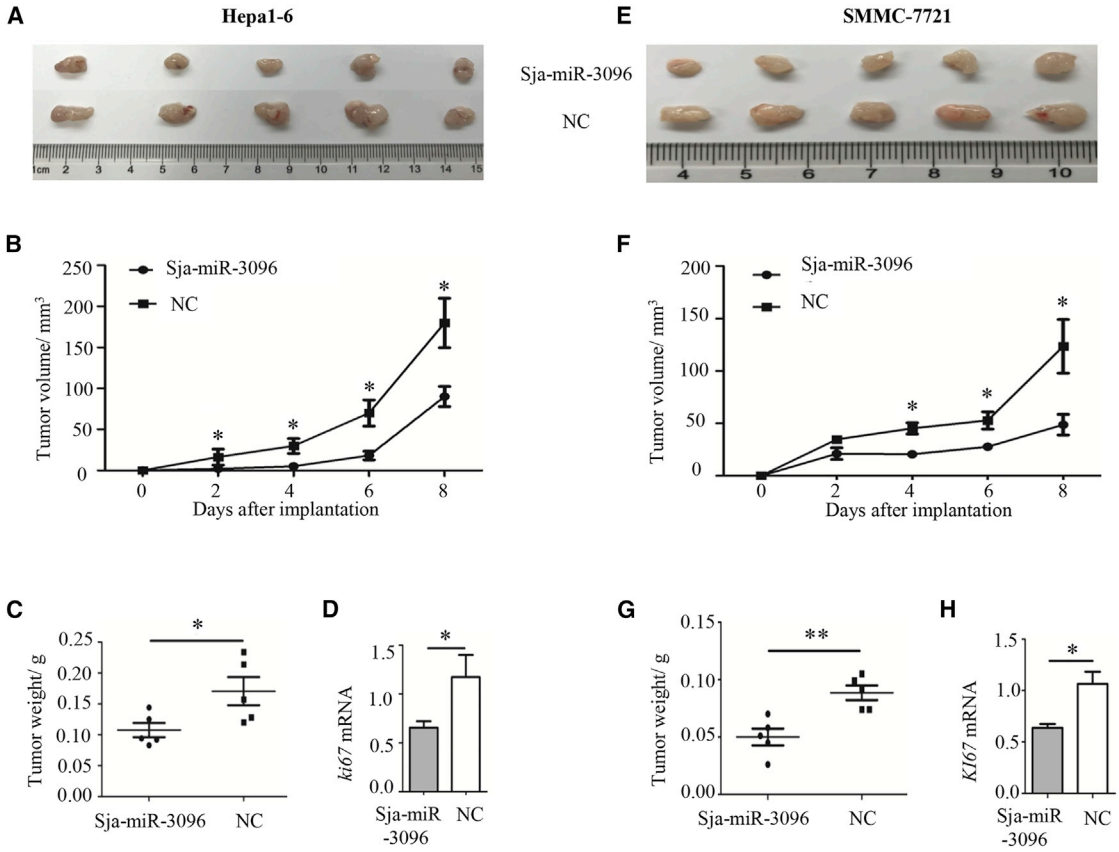

Figure 3. Inhibitory Effect of Sja-miR-3096 on Hepatoma Cell Growth *In Vivo*

The Hepa1-6 cells (A–D) and SMMC-7721 cells (E–H) transfected with Sja-miR-3096 or NC mimics were subcutaneously implanted per flank of nude mice and the mice were sacrificed 8 days later. (A and E) Tumor images were prepared at day 8 after implantation of hepatoma cells transfected with Sja-miR-3096 (upper) or NC mimics (lower) (n = 5). (B and F) The tumor volume was measured at days 2, 4, 6, and 8 after injection. (C and G) Tumors were weighed in the mice of the two groups at day 8. (D and H) The mRNA level of *KI67* was measured in the tumors derived from the mice in Sja-miR-3096 or NC mimics group. The experiments were performed in triplicate. Data are expressed as mean ± SEM values (*$p < 0.05$, **$p < 0.01$). See also Figure S6.

on day 8 after injection (Figure S6A), and the mRNA level of *ki67* (a tumor proliferation marker) was significantly downregulated in -tumor cells transfected with Sja-miR-3096 compared to that with NC (Figure 3D). Similar results were obtained with the human cell line of SMMC-7721 (Figures 3E–3H; Figure S6B). These data indicated that Sja-miR-3096 suppressed both murine and human hepatoma cell growth *in vivo*.

Cross-Species Processing of Sja-miR-3096 and Its Effect on Hepatoma Cell Growth *In Vivo*

To investigate the effect of Sja-miR-3096 produced in hepatoma cells, we constructed a recombinant plasmid expressing pri-Sja-miR-3096 gene by inserting a 450-bp fragment of pri-Sja-miR-3096 into the pLVX plasmid (designated as pLVX-3096). Transient transfection of the recombinant plasmid into the Hepa1-6 cells led to the expression of both pri- and mature Sja-miR-3096 by qRT-PCR (Figures 4A–4C), and it also confirmed the sequence of mature Sja-miR-3096 through cloning and sequencing (Figure S7A), indicating that the schistosome pri-miRNA could be properly processed in mammalian cells. We generated a Hepa1-6 cell line (designated as Hepa1-6/3096) that stably expresses the pri- and mature Sja-miR-3096 detected by qRT-PCR (Figures S7B–S7D). To further confirm the cross-species processing and evaluate expression abundance of the mature Sja-miR-3096 in the stable cell line, small RNA (<30 nt) extracted from the Hepa1-6/3096 stable cell line was sequenced by Illumina deep sequencing technology, yielding 31,634,744 clean reads that were mainly distributed between 20∼24 nt in length (Figure S7E; Figure 4D). Of them, 11,899,682 reads were mapped to 952 known murine miRNAs (Table S1). Abundances of the miRNAs varied from 1 to 3,446,386 reads, with an average of 12,500 reads per miRNA. Of the 952 murine miRNAs, 44% have ≤9 reads while 32% have >100 reads (Figure 4E). We identified 10 reads of mature Sja-miR-3096 in the Hepa1-6/3096 stable cell line through the sequence alignment (Table S2). Thus, these data indicated that the schistosome pri-miRNA can be properly processed in the mammalian cell and yielded the mature Sja-miR-3096.

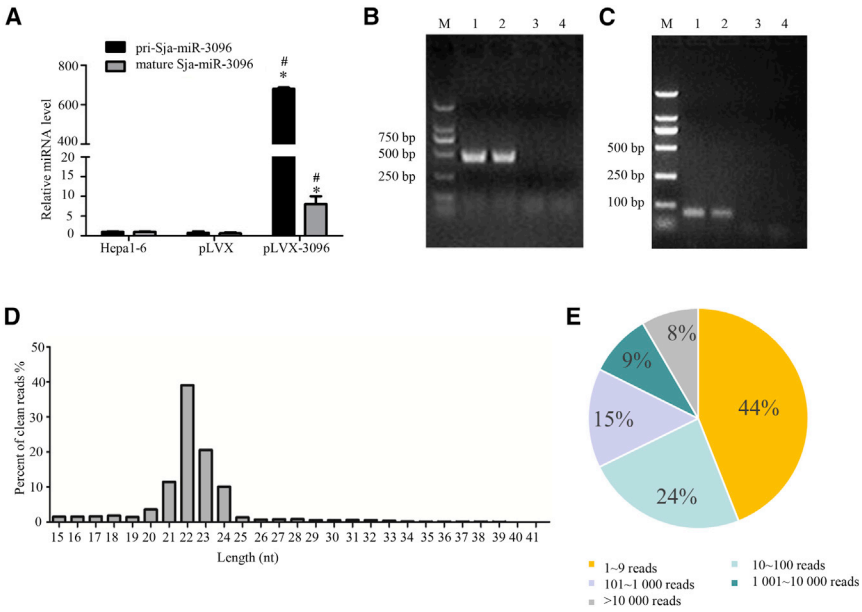

Figure 4. Cross-Species Processing of Sja-miR-3096

(A) Total RNAs were extracted from the Hepa1-6 cells transiently transfected with empty plasmid pLVX or the recombinant plasmid pLVX-3096 and detected for the expression of pri-Sja-miR-3096 and mature Sja-miR-3096 by qRT-PCR. Detection of PCR products by 2% agar gel electrophoresis for the pri-Sja-miR-3096 (B) and mature Sja-miR-3096 (C). Lane 1, positive control (qRT-PCR products from recombinant plasmid pLVX-3096 template) (B), whereas qRT-PCR products are from Sja-miR-3096 mimics cDNA template (C); qRT-PCR products of Hepa1-6 cells transfected with pLVX-3096 (lane 2) and pLVX empty plasmid (lane 3); and lane 4, qRT-PCR products of Hepa1-6 cells. $^{*}p < 0.05$ compared to pLVX group; $^{\#}p < 0.05$ compared to Hepa1-6 group (A). The data are presented as the mean ± SEM of three independent experiments. (D and E) Sequencing data of small RNA of Hepa1-6/3096 cells. (D) Length distribution of clean reads. (E) Abundance distribution of murine-derived miRNAs. The 952 murine miRNAs were divided into five groups based on their abundance: 1–9, 10–100, 101–1,000, 1,001–10,000, and >10,000 reads. See also Figure S7.

Subsequently, we evaluated the effects of the intracellular production of the heterogeneous Sja-miR-3096 miRNA on hepatoma cell growth. FACS analysis of Hepa1-6/3096 cells revealed that the cell cycle was largely arrested at the G_0/G_1 phase (Figure 5A), and the cell proliferation was highly suppressed in the Hepa1-6/3096 cells compared to the control cells (Figure 5B). Furthermore, significant inhibition of colony formation was observed in the Hepa1-6/3096 cell line compared to the control cell lines (Figure 5C; Figure S8). These data indicate that the low level of intracellular Sja-miR-3096 exerts a notable anticancer activity *in vitro*.

To investigate the effect of the intracellular Sja-miR-3096 on tumorigenesis of Hepa1-6/3096 cells *in vivo*, Hepa1-6/3096 and Hepa1-6/pLVX (as NC) cells were placed into the left and the right scapula of each mouse, respectively (n = 12), for subcutaneous inoculation. As shown in Figure 5D, the tumors were detectable on day 3, and after that they rapidly grew in size in the mice inoculated with the control cells. In contrast, no solid tumor was detected throughout the observation period in the mice inoculated with the Hepa1-6/3096 cells. At day 10 after implantation, all mice were sacrificed and the tumors were removed for measurement (Figure 5E). Again, no solid tumor was found in the mice inoculated with the Hepa1-6/3096 cells, while solid tumors were found in the mice inoculated with the control cells (Figure 5F).

We further evaluated the antitumor effect of the intracellular Sja-miR-3096 in a murine orthotopic transplantation liver tumor model. Both Hepa1-6/3096 and control cells were transplanted into the liver of mice (n = 5). As shown in Figures 5G–5I, tumors were observed in the livers of all mice transplanted with the control cells and also in the abdomen of some mice in this group, which was probably caused by leakage of cells during the orthotopic implantation. In contrast, no solid tumor was detected in both the liver and abdomen of the mice inoculated with the Hepa1-6/3096 cells. In addition, the weight of the liver was significantly higher in the control group than in the Hepa1-6/3096 group (Figure 5J). These data indicate that sustained production of intracellular Sja-miR-3096, despite a low level, completely suppressed tumorigenesis of hepatoma cells *in vivo*.

Evaluation of the Antitumor Activity through Intravenous Injection of Sja-miR-3096 Mimics

The antitumor effect of Sja-miR-3096 mimics was further evaluated in mice bearing Hepa1-6 xenografts by intravenous injection. To this end, the Hepa1-6 cells were s.c. implanted into the right and left scapula of nude mice, followed by intravenous injection of Sja-miR-3096 mimics, NC or PBS, respectively, mixed with the *in vivo* transfection reagent daily for 4 days. As shown in Figure 6A, the tumor weights were significantly reduced in the mice inoculated with the Sja-miR-3096 mimics compared to that with the NC and PBS. Furthermore, immunohistochemical analysis showed that the percentage of cells positive for KI67 (a tumor proliferation marker) was also significantly decreased in the Sja-miR-3096-treated mice compared to that in the control mice (Figures 6B and 6C). In addition, daily measurement of tumor volumes showed that the lowest volumes were consistently observed in the mice inoculated with the Sja-miR-3096 mimics (Figure 6D). The injected Sja-miR-3096 mimics were detectable in the tumors on day 5 after implantation (Figure S9A). These data indicate that Sja-miR-3096 mimics via intravenous administration generated inhibitory effects on the growth of the hepatoma cells *in vivo*. To assess any toxic side effects of the treatment with the miRNA mimics, we measured the serum alanine aminotransferase (ALT) levels and the weights of vital organs of the treated mice. There were no substantial differences between the groups (Figures S9B and S9C).

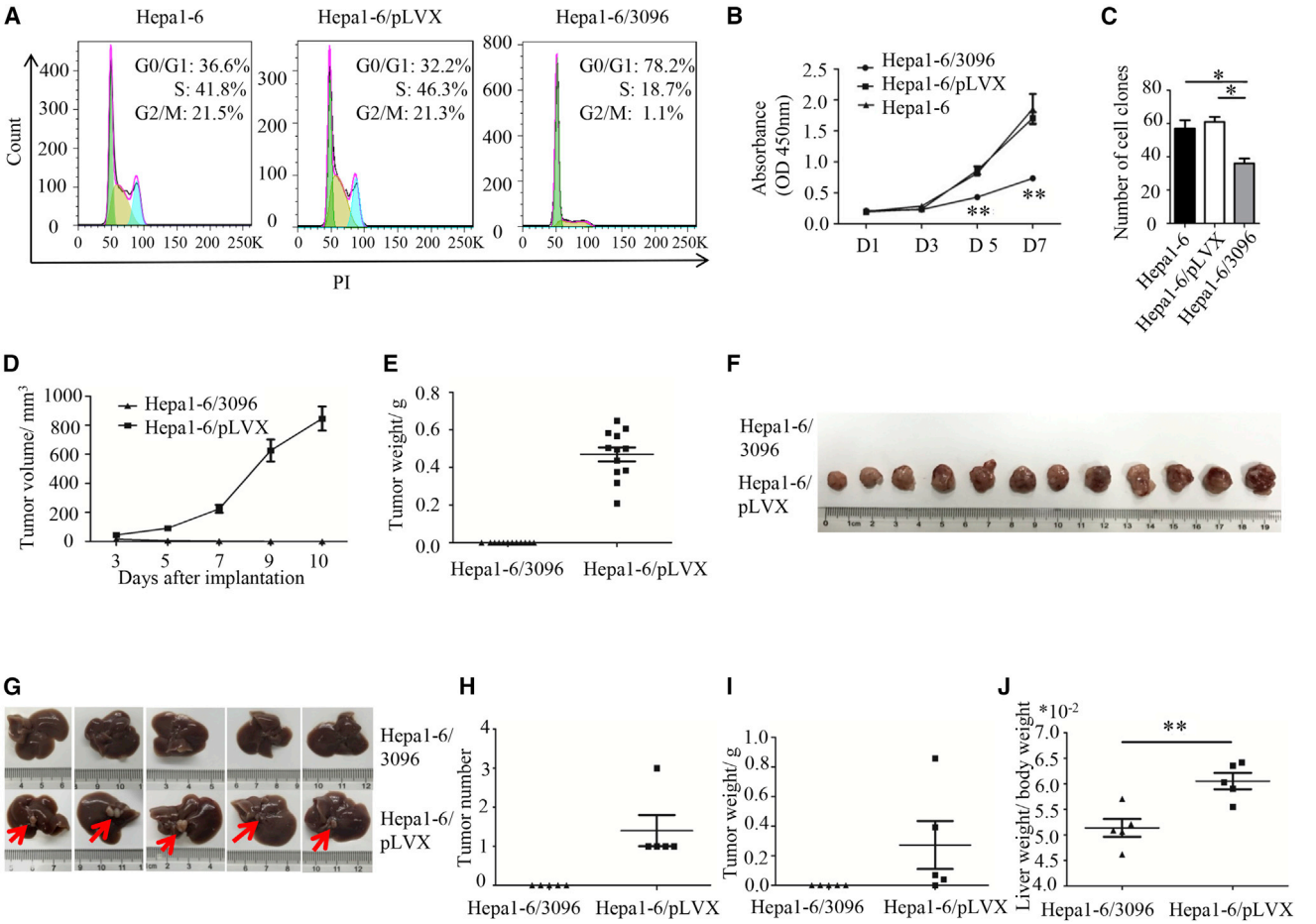

Figure 5. Antitumor Effect of Intracellular Production of Sja-miR-3096

The stable hepatoma cell that constitutively produces mature Sja-miR-3096 showed cell cycle arrest at the G_0/G_1 phase (A), suppression of cell growth (B), and colony formation (C). **p < 0.01, compared to Hepa1-6/pLVX or Hepa1-6 group, respectively (B). (D–F) Tumorigenesis of the stable cell lines in a subcutaneous xenograft of mice. (D) The tumor growth curve was measured every 2 days for 10 days after inoculation (n = 12). The tumor mass (E) and tumor images (F) obtained from the sacrificed mice on day 10 after inoculation are shown. (G–J) Tumorigenesis of the stable cell lines in a murine orthotopic liver tumor model. The stable cells were transplanted into the liver of mice (n = 5). Three weeks after implantation, the mice were sacrificed and representative liver images are shown (G) together with the number of tumors in the livers (H) and weights of tumors in the abdomen (I) and body and livers (J). The experiment was performed in triplicate. Data are shown as the mean ± SEM values (*p < 0.05, **p < 0.01). See also Figure S8.

Antitumor Effect of Sja-miR-3096 by Targeting *PIK3C2A*

To elucidate the molecular mechanisms underlying the inhibitory effect of Sja-miR-3096 on hepatoma cell growth, we performed a computational analysis to search for putative targets of this miRNA using miRDB. Six genes, including *N*-myristoyltransferase 1 (*NMT1*), tet methylcytosine dioxygenase 3 (*TET3*), and *PIK3C2A*, were predicted as target gene candidates for murine and human cells according to the higher predicted scores and potential involvement in the tumor-related signaling pathway. However, five of them (except for *PIK3C2A* gene) were excluded through analysis of their expression in hepatoma cells transfected with Sja-miR-3096 mimics. Thus, the *PIK3C2A* gene was selected as being a predicted target of Sja-miR-3096 for further analysis. There are two sites, T1 and T2, found in the 3′ UTR of the murine *Pik3c2a* gene (Figure 7A) and one site (T3) in the human *PIK3C2A* gene (Figure 7B). To validate the relationship between Sja-miR-3096 and *PIK3C2A*, we first generated two constructs: pmirGLO-WT, the firefly luciferase gene fused to the 450-bp 3′ UTR fragment of *Pik3c2a*, including T1 and T2, and pmirGLO-MT, a construct with seven mutation nucleotides in the seed region (Figure 7A), and similar constructs for *PIK3C2A* (Figure 7B). The constructs together with the miRNA mimics were transiently transfected into Hepa1-6 cells or SMMC-7721 cells, and the relative luciferase activity was assessed. As shown in Figure 7C, the luciferase activity was significantly reduced in the cells transfected with the pmirGLO-WT, whereas the mutations in the seed sequence completely abrogated the inhibitory effect on reporter expression. Furthermore, transfection of the Sja-miR-3096 mimics into the Hepa1-6 and SMMC-7721 cell lines, respectively,

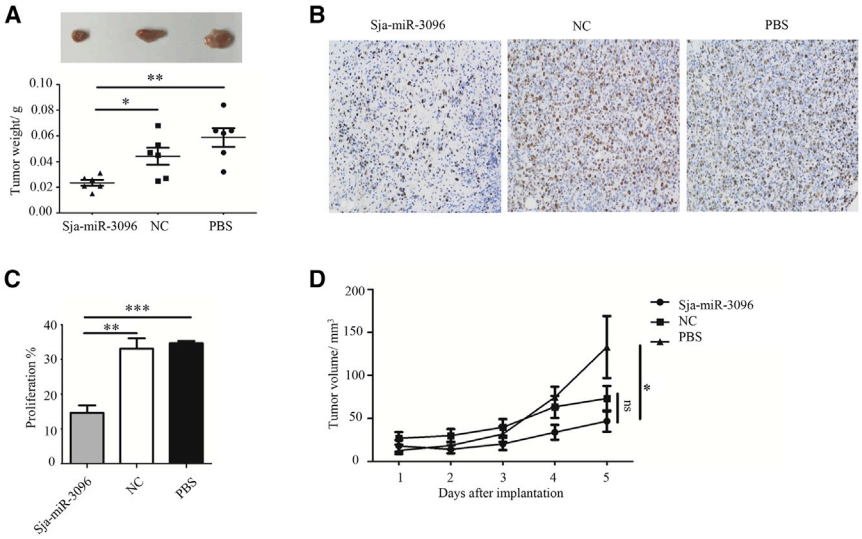

Figure 6. The Antitumor Effect of Intravenous Injection of Sja-miR-3096 Mimics

Hepa1-6 cells were subcutaneously implanted per flank of nude mice and then the mice received an intravenous injection of the Sja-miR-3096, NC mimics, or PBS mixed with *in vivo* transfection reagent. (A) The mass of tumors obtained from different groups were weighted. (B and C) Immunohistochemical analysis of KI67 expression was performed. (D) Tumor volumes were measured at various time points. Data are presented as mean ± SEM of three independent experiments (n = 6) (*$p < 0.05$, **$p < 0.01$, ***$p < 0.001$, ns, no statistical significance). See also Figure S9.

led to a reduction in expression of the *PIK3C2A* (Figures 7D–7F). We also showed that expression of PIK3C2A protein was completely inhibited in the Hepa1-6/3096 stable cell line (Figure 7G). In addition, the protein level of the PIK3C2A was significantly decreased in tumor tissues receiving Sja-miR-3096 mimics compared to those receiving NC (Figure S10). These results indicate that both murine *Pik3c2a* and human *PIK3C2A* genes are the direct target of Sja-miR-3096.

Involvement of *PIK3C2A* in Sja-miR-3096-Mediated Antitumor Activity

Previous studies have shown that *PIK3C2A* plays crucial roles in vascular formation, barrier integrity, and platelet membrane morphology.[23,24] To investigate whether Sja-miR-3096 inhibits the growth and migration of hepatoma cells by repressing *PIK3C2A* expression, both Hepa1-6 cells and SMMC-7721 cells were transiently transfected with Sja-miR-3096 mimics or corresponding *PIK3C2A* small interfering RNA (*PIK3C2A* siRNA). As shown in Figure 8A, *PIK3C2A* siRNA significantly reduced both murine and human *PIK3C2A* expression at both the transcriptional and translational levels, as detected by qRT-PCR and Western blot, respectively. Furthermore, Western blot analysis revealed that p-mTOR (Ser^{2448}), one of the key downstream nodes in *PIK3C2A* signaling pathway, was downregulated in both Hepa1-6 and SMMC-7721 cells transfected with either Sja-miR-3096 mimics or the *PIK3C2A* siRNA compared with that in the NC-treated cells (Figure 8B). The *PIK3C2A* siRNA-mediated downregulation of *PIK3C2A* and its downstream node p-mTOR (Ser^{2448}) led to the cell cycle arrest at the G_0/G_1 phase (Figure S11A), inhibition of cell proliferation (Figure 8C), cell migration (Figure 8D), and colony formation (Figure 8E; Figure S11B) similar to the phenotype of the Sja-miR-3096-treated cells, suggesting that Sja-miR-3096 exerts its antitumor effects by targeting *PIK3C2A* to reduce the expression of p-mTOR (Ser^{2448}), resulting in suppression of hepatoma cell proliferation and migration.

DISCUSSION

The present study demonstrates that a schistosome miRNA, Sja-miR-3096, which is also present in host liver cells during the infection, has notable inhibitory effects on the growth and migration of tumor cells via cross-species regulation of host tumor-related genes, based on the following findings: (1) *in vitro* transfection of the synthetic Sja-miR-3096 into hepatoma cells led to inhibition of cell proliferation, colony formation, and cell migration; (2) complete suppression of tumorigenesis of a stable hepatoma cell line that constitutively produces intracellular mature Sja-miR-3096 when inoculated into both scapulae and livers of mice; and (3) intravenous injection of Sja-miR-3096 mimics had an inhibitory effect on the tumor growth in mice bearing hepatocellular carcinoma xenografts. Mechanistically, Sja-miR-3096 suppresses tumor cell growth and migration by targeting *PIK3C2A* and thereby downregulation of mTORC1. In addition, we demonstrated cross-species processing of the schistosome pri-miRNA to mature Sja-miR-3096 in mammalian cells.

It is well documented that infection with certain pathogenic species such as human papillomavirus, hepatitis B virus (HBV), and *Helicobacter pylori* is associated with cancers.[25–27] Among parasitic diseases, infections with *Clonorchis sinensis* and *Schistosoma haematobium* have been reported to be associated with cancers.[28,29] In the case of *S. japonicum* infection, no convincing evidence demonstrated the association between schistosome infection and hepatocellular cancer (HCC), although this disease was widespread and affected tens of millions of people in the past.[30] Two large retrospective epidemiological surveys conducted in China, one national and the other conducted in seven counties that are highly endemic for schistosomiasis, showed that there was no correlation between *S. japonicum* infection and HCC.[31,32] Although several epidemiological and case-control studies proposed the association of *S. japonicum* schistosomiasis with HCC, the evidence for the positive association remains debated because the schistosomiasis patients, particularly the advanced patients, are highly associated with HBV and hepatitis C virus (HCV) infections that are hepatic carcinogens.[33] Accumulating evidence indicated that chronic inflammation plays an important role in carcinogenesis and could be involved in promoting tumor growth, tissue

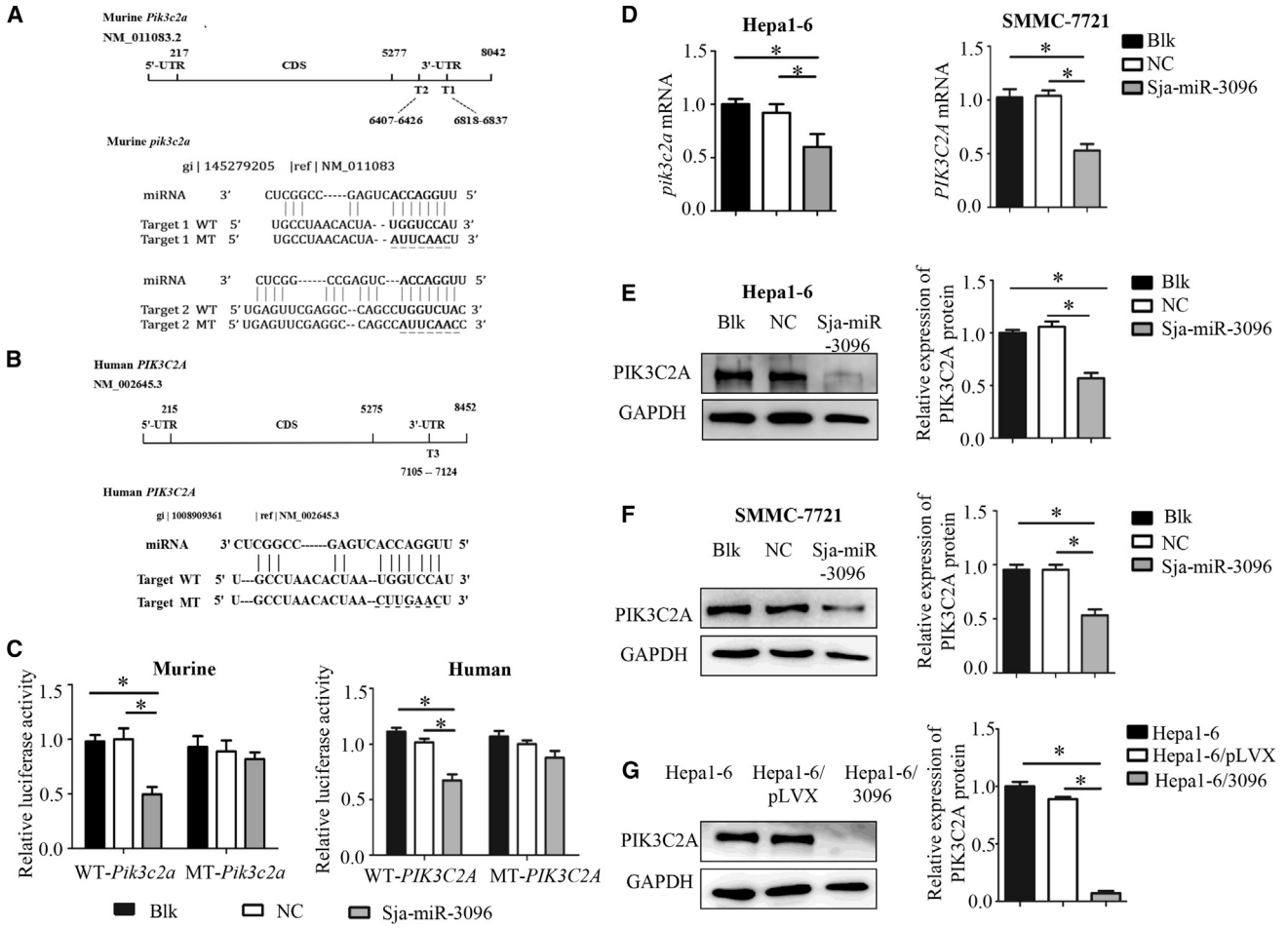

Figure 7. The Target of Sja-miR-3096

(A) Structure of the murine *Pik3c2a* gene. There are two putative Sja-miR-3096-binding sites located at its 3′ UTR (upper panel). Sequence of wild-type (WT) and mutant-type (MT) Sja-miR-3096 target sites and comparison of their seed sequence with the miRNA sequence (lower panel). (B) Structure of the human *PIK3C2A* gene. One putative Sja-miR-3096-binding site was located at the 3′ UTR of the gene (upper panel). Sequence of WT and MT Sja-miR-3096 target sites and comparison of their seed sequence with the miRNA sequence (lower panel). Luciferase reporter assay: (C) Hepa1-6 and SMMC-7721 cells were co-transfected with luciferase reporter plasmids containing WT or MT Sja-miR-3096 target sites and Sja-miR-3096 or NC mimics. *PIK3C2A* expression was detected by qRT-PCR (D) and Western blot (E and F) analysis in the Hepa1-6 (E) and SMMC-7721 (F) cells transfected with synthetic Sja-miR-3096 or NC. (G) PIK3C2A expression was detected by Western blot in the stable cell line. All results were derived from independent experiments performed in triplicate. Data are presented as the mean ± SEM (*$p < 0.05$). See also Figure S10.

invasion, and metastasis.[34–36] For *S. japonicum* infection, the liver-trapped eggs of *S. japonicum* induce severe hepatic chronic inflammation and fibrosis that could be a risk factor for HCC as a result of DNA damage and somatic mutation of genes that were observed in other cancers.[37,38] In addition, egg-induced fibrosis could also be a risk factor for carcinogenesis by alteration of proliferation, hyperplasia, and metaplasia.[39] These factors derived from *S. japonicum* infection could contribute to HCC, but this does not seem to happen in the *S. japonicum* schistosomiasis. We speculated that the *S. japonicum* eggs trapped in the liver might play a dual role in the HCC occurrence and development, i.e., carcinogenic and anticancer activities, similar to those reported for the protozoan *Trypanosoma cruzi*, which has carcinogenic and anticancer properties during infection.[40] This study demonstrated that a noncoding small RNA secreted by *S. japonicum*, Sja-miR-3096, can be translocated into liver cells during the parasite infection and inhibits tumor cell growth and migration, implying that the factors derived from *S. japonicum* may contribute to anticancer activities in the infected host.

Studies have revealed that small RNAs are not limited to the individual in whom they are produced, but they show cross-kingdom influences through communication between hosts and more advanced pathogens such as parasites, thus leading toward inter-organismic gene silencing.[41,42] miRNAs are transcribed as long primary transcripts (pri-miRNAs) that are processed to mature miRNAs through sequential processing events: the nuclear processing of the pri-miRNAs into stem-loop precursors of ~70 nucleotides (pre-miRNAs), and the cytoplasmic processing of pre-miRNAs into mature

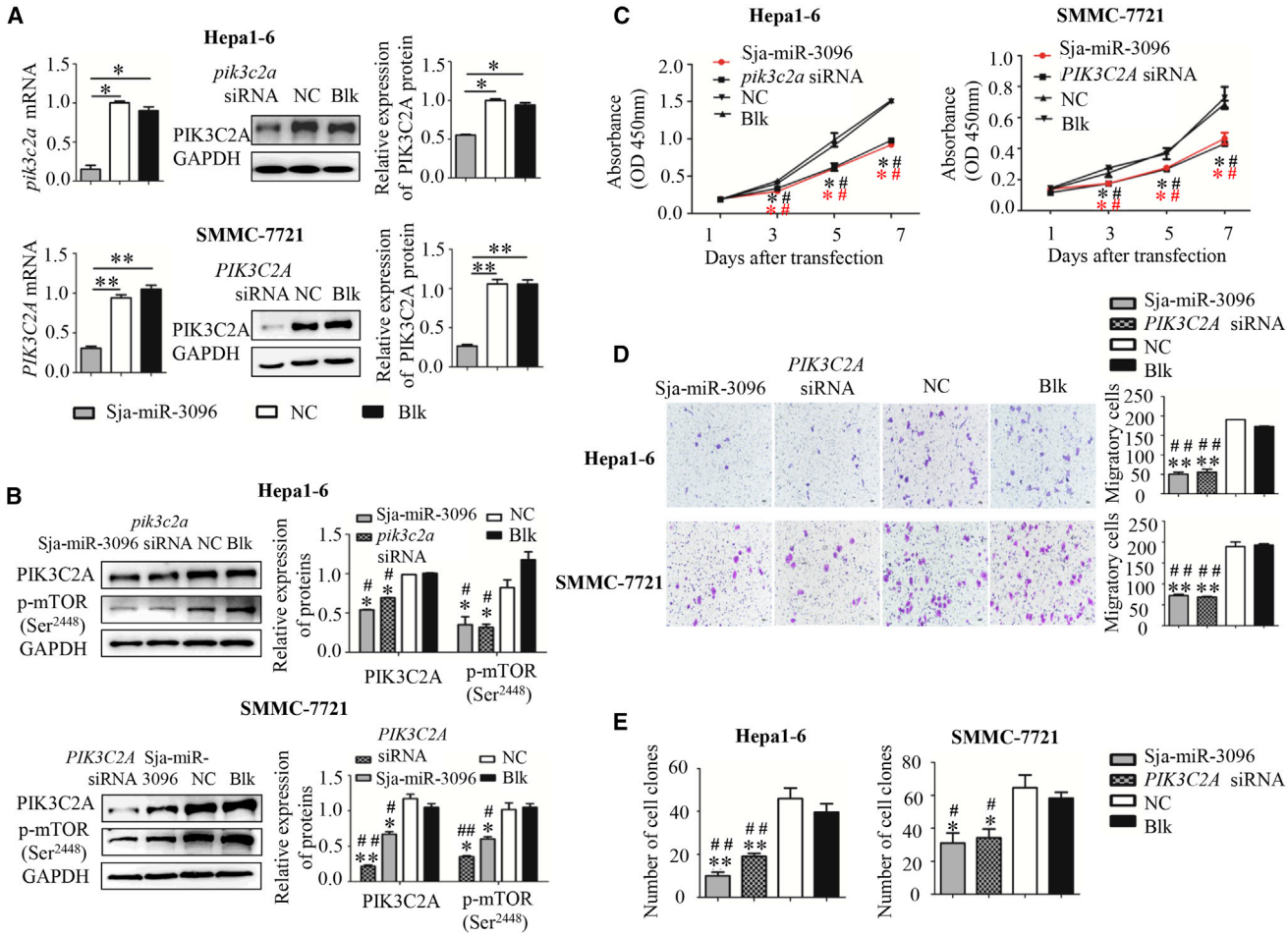

Figure 8. Knockdown of *PIK3C2A* Inhibits Cell Proliferation and Migration of Hepatoma Cells *In Vitro*

Hepa1-6 and SMMC-7721 cells were transfected with murine or human *PIK3C2A* siRNA and NC siRNA, respectively, and 48 h later, the expression of *PIK3C2A* was determined using qRT-PCR and Western blotting to identify the efficiency of murine or human *PIK3C2A* siRNA (A). (B–E) Hepa1-6 and SMMC-7721 cells were transfected with Sja-miR-3096 mimics, murine or human *PIK3C2A* siRNA, and NC, respectively. (B) Western blot detection of expression of PIK3C2A and p-mTOR (Ser2448) in the treated hepatoma cells and quantified data. (C) Cell proliferation was evaluated using the CCK-8 assay at days 1, 3, 5, and 7. Data are presented as the mean ± SEM. #$p < 0.05$, Sja-miR-3096 compared to Blk; *$p < 0.05$, Sja-miR-3096 compared to NC; #$p < 0.05$, PIK3C2A siRNA compared to Blk; *$p < 0.05$, PIK3C2A siRNA compared to NC (C). (D) Cell migration was evaluated by the transwell migration assay. (E) The ability to form cell clones was determined using a colony formation assay. Data are presented as the mean ± SEM. #$p < 0.05$ versus Blk, *$p < 0.05$ versus NC (B, D, and E). All results were derived from independent experiments performed in triplicate. See also Figure S11.

miRNAs.[1] The efficiency of this maturation processing is mainly affected by the secondary structure of miRNAs rather than their nucleic acid sequence, particularly in the nuclear processing completed by an RNase III endonuclease, Drosha,[43,44] which provides a possibility of cross-species processing of miRNAs. Recently, several studies have observed the cross-species processing of miRNAs. RV-vsRNA1755, a rotavirus-encoded miRNA, can be properly processed into mature miRNA in gene-transfected or virus-infected mammalian cells.[45] Also, plant pre-miR-168a was properly processed in mammalian HepG2 cells.[10] In this study, we demonstrated for the first time that a parasite pri-miRNA is processed to the mature Sja-miR-3096 in mammalian cells. Importantly, we found that a low level of the mature Sja-miR-3096 produced in cells exerts considerable anticancer effects in an across-species manner, which could provide a possibility of a vector-mediated delivery of such parasite pri-miRNAs into mammalian target cells as a therapeutic intervention for human diseases such as cancers.

This study found that Sja-miR-3096 inhibits growth and migration of both murine and human hepatoma cells by targeting the *PIK3C2A* gene, which encodes for one of the members of the class II PI3K subfamily (C2α). With regard to the involvement of *PIK3C2A* in modulation of tumor cell proliferation, Ng et al.[46] reported that elevated *PIK3C2A* expression was detected in tissue samples of hepatitis B virus–positive hepatocellular cancers. Moreover, Yoshioka et al.[24] demonstrated that endothelial cell-specific deficiency of

Pik3c2a in mice resulted in markedly reduced retinal angiogenesis and also a decrease in the overall volume of solid tumors that were implanted in the mice. In addition, it has been reported that *PIK3C2A* regulates the migration and invasion of various types of cancer cells.[47,48] These observations indicate that *PIK3C2A* is involved in carcinogenesis and development of cancer.

It is generally accepted that the classical phosphatidylinositol 3-kinase (PI3K) pathway is involved in cancer occurrence and progression through modulation of downstream nodes such as mTORC1.[49] Furthermore, the mTORC1 participates in the regulation of tumor cell growth and migration.[50–52] Similarly, in this study we showed that Sja-miR-3096-mediated downregulation of PIK3C2A also reduced expression of p-mTOR (Ser^{2448}), leading to inhibition of growth and migration of hepatoma cells. Thus, the discovery and development of such heterogeneous antitumor miRNAs may present a promising therapeutic intervention for liver cancers.

MATERIALS AND METHODS

Cell Lines and Culture

The Hepa1-6, NCTC-1469, SMMC-7721, Raw264.7, and L929 cell lines were obtained from American Type Culture Collection (ATCC). All of these cell lines were cultured according to the standard protocol for DMEM (Life Technologies, USA) supplemented with 10% fetal bovine serum (FBS; Life Technologies, USA), 100 U of penicillin, 100 μg/mL streptomycin, and 0.25 μg/mL amphotericin B (Life Technologies, USA) in a 37°C incubator containing 5% CO_2.

Cell Viability Assay

Cell viability was evaluated by CCK-8 (Dojindo, Kumamoto, Japan). Hepa1-6 cells transfected with miRNAs or NC mimics were seeded in 100 μL of DMEM at a density of 5×10^3 cells/well in 96-well plates. After 48 h, 10 μL of CCK-8 was added and the culture was continued for 20 min at 37°C. The absorbance was read at a wavelength of 450 nm with an automated plate reader. Wells containing the CCK-8 reagents without cells were used as the Blk. Cell viability was expressed as a percentage relative to control cells. Cell proliferation was assessed based on the absorbance values according to the manufacturer's protocol. In brief, Hepa1-6 cells and SMMC-7721 cells were seeded into 96-well plates at 2×10^3 cells/well and transfected with 40 nM Sja-miR-3096, murine or human *PIK3C2A* siRNA, or NC mimics. CCK-8 reagent was added and absorbance was read just as described above at four time points of days 1, 3, 5, and 7.

Cell Cycle Measurement

Hepa1-6 cells were transfected with 40 nM miRNA, murine *pik3c2a* siRNA, or NC mimics, collected after 48 h, and stained with propidium iodide (PI; Beyotime, China) for cell cycle analysis with FACS (BD Biosciences, USA). Data were collected and analyzed with FlowJo software.

Transwell Migration Assays

Transwell assays were performed with Corning transwell inserts in accordance with the manufacturer's instructions. The upper chambers were seeded with 100 μL (1×10^4 cells) of hepatoma cells transfected with miRNA, siRNA, or NC mimics, respectively, whereas the lower chambers were filled with DMEM. Cells were allowed to migrate from the upper to the lower chambers. Cells attached to the lower surface of the membrane were fixed and counterstained with crystal violet, and the number was counted under the microscope. A total of five fields were counted for each transwell filter.

Library Preparation, Sequencing, and Analysis for Small RNA

The Hepa1-6/3096 RNA samples were sent to Shanghai Oebiotech (Shanghai, China) for small RNA library construction and sequencing. The libraries were constructed as previously described.[53,54] Briefly, a total of 1.5 μg of RNA per sample was used for the construction of sequencing libraries. Library quality was assessed using the Agilent Bioanalyzer 2100 (Agilent Technologies, Palo Alto, CA, USA). Library preparations were then sequenced on an Illumina HiSeq 2500 platform (Illumina, Santa Clara, CA, USA) and paired-end reads were generated.

The data were analyzed as previously described.[55] Briefly, after removing low-quality reads, adaptors, insufficient tags, and sequences, the length distributions of the clean reads were summarized. The tRNAs, small nuclear RNAs (snRNAs), rRNAs, and other noncoding RNAs were removed based on comparisons with the GenBank and Rfam databases. The count of Sja-miR-3096 was obtained by aligning mature Sja-miR-3096 sequence to the remaining clean reads. Known murine-derived miRNAs were divided into five groups based on abundance (1–9, 10–100, 101–1,000, 1,001–10,000, and >10 000 reads), and the abundance distribution was summarized by calculating the percentage of miRNAs in each group as a percentage of total known murine-derived miRNAs.

Western Blot Detection

Protein lysates were extracted and ~20 μg of protein was separated by 10% SDS-PAGE and transferred to a nitrocellulose membrane. Then the membrane was blocked with 5% BSA in Tris-buffered saline with Tween 20 (TBST) for 2 h at room temperature, followed by incubation overnight with primary antibodies, including those to PIK3C2A and p-mTOR (Ser^{2448}) that were purchased from Cell Signaling Technology (USA) and heat shock protein (HSP)90 that was purchased from Proteintech (Wuhan, China). After incubating with the relevant secondary antibodies (Promega, USA), the membranes were visualized by using the ECL reagent (GE Healthcare, UK), and the protein bands were subsequently measured using the ImageQuant LAS 4000mini (GE Healthcare, USA). Gray analysis with ImageJ and data were quantified to glyceraldehyde-3-phosphate dehydrogenase (GAPDH).

Infection of Mice with *S. japonicum* Cercariae

Animal experiments were performed in accordance with the *Guide for the Care and Use of Laboratory Animals* of the National Institutes of Health and approved by the Internal Review Board of Tongji University School of Medicine. The animal surgeries were undertaken under sodium pentobarbital anesthesia. Cercariae of *S. japonicum* were provided by the National Institute of Parasitic Disease, Chinese

Center for Disease Control and Prevention (CDC). Six-week-old male C57BL/6J mice (18–20 g), purchased from the experimental animal center of the Second Military Medical University and housed under specific pathogen-free conditions, were percutaneously infected with 50 or 100 cercariae of *S. japonicum* per mouse (50 for collection of infected hepatocytes and 100 for collection of early-stage parasites).

For collection of parasites, the hepatic schistosomula were isolated from the portal system and mesenteric veins of infected mice at 7 and 14 days postinfection (dpi). Also, adult worms of *S. japonicum* were isolated from the hepatic portal system and mesenteric veins at 42 dpi. Male and female adult worms were manually separated under a light microscope. The eggs were isolated with a traditional method, as described by Cai et al.[56] All freshly isolated parasites were washed three times with PBS (pH 7.4) and were immediately used for extraction of total RNA or frozen at −80°C until being subjected to further analysis.

Isolation of Primary Mouse Hepatocytes

The primary mouse hepatocytes were isolated by a two-step collagenase perfusion procedure, as described by He et al.[57] with minor modifications. Briefly, livers of the infected mice were initially *in situ* digested with 0.03% collagenase type IV and then further digested with 0.08% collagenase type IV at 37°C. The single-cell suspensions were harvested by filtration through 400-mesh sieves for removal of the remaining tissue debris and parasite eggs. Next, hepatocytes were isolated by centrifugation of the resulting cell suspensions at 50 × *g* for 4 min and further purified by centrifugation at 20 × *g* for 4 min. Purified hepatocytes were resuspended in DMEM containing 20 μg/mL ribonuclease A (Sigma-Aldrich, USA) at 37°C for 30 min to eliminate any miRNA that might be released by schistosomes and adhere to the surface of hepatocyte. After washing with PBS three times, the cell pellet was immediately used for extraction of total RNA or frozen at −80°C until used.

Isolation and Characterization of Exosome-Like Vesicle

An exoEasy Maxi kit from Qiagen (Hilden, Germany) was used for exosome isolation according to the supplier's protocols. The methods of *S. japonicum* egg isolation, culture, and culture medium collection were described in Zhu et al.[17]

For characterization of exosome-like vesicles, the particle size distribution was determined by Malvern nanoparticle analysis (Malvern Panalytical, UK). Purified EVs were applied to 200-mesh Formvar-coated electron microscopy (EM) grids (Agar Scientific, Essex, UK). The grids were stained with 1% uranyl acetate (System Biosciences) for 5 min and then loaded onto the sample holder of the JEM-1230 transmission electron microscope (JEOL, Tokyo, Japan) and exposed to an 80-kV electron beam for image capture. The protein concentration of the purified EV sample was determined by an enhanced BCA protein assay kit (Beyotime, China). Then, 200 μL of the EV sample was added to 1 mL of TRIzol (Invitrogen, USA), and 20 nmol of cel-miR-39 mimics was added as an external control for quantitative detection. 4 μg of total RNA was extracted for subsequent qRT-PCR to detect the Sja-miR-3096 content. Moreover, the expression of HSP90,[58] a typical EV marker, was detected by western blot.

Hepatocellular Carcinoma Xenografts

Transfection with Synthetic miRNA Mimics

Hepa1-6 and SMMC-7721 cells were transfected with Sja-miR-3096 mimics or NC mimics at a final concentration of 80 nM. 24 h later, the transfected cells were s.c. implanted (2×10^6 cells in 100 μL of PBS) per flank of male BALB/c nude mice (4 weeks old). The tumor volumes were measured by vernier caliper at days 2, 4, 6, and 8 after implantation, and the mice were euthanized at day 8. The total RNA of tumors was isolated using TRIzol reagent for detecting the expression of *KI67* mRNA and Sja-miR-3096. The protein of tumors was prepared for detecting the expression of PIK3C2A.

Stable Cell Lines

Hepa1-6/3096 or Hepa1-6/pLVX stable cells (5×10^6 cells) in 100 μL of PBS were s.c. implanted to the double flanks of 12 BALB/c nude mice to obtain subcutaneous tumors. For the orthotopic transplantation mice model, ten 5-week-old C57BL/6J male mice were randomized into two groups and 25 μL (1×10^6 cells) of Hepa1-6/3096 or control cells was *in situ* implanted into the mice liver. The mice were sacrificed after 3 weeks. The tumors on livers were counted and the mice body, livers weights, and tumors in the abdomen were measured by electronic balance.

Immunohistochemistry

To determine KI67 expression in xenograft tumor tissues from the athymic nude mice, immunohistochemistry (IHC) was performed as described previously[59]. Antibody against KI67 was used (1:50 dilution).

Statistical Analysis

Results were analyzed using GraphPad Prism 5.0 software (GraphPad Software, La Jolla, CA, USA), and statistical analyses were performed using a two-tailed Student's t test. A value of $p < 0.05$ was considered statistically significant. Data are expressed as mean ± SEM.

SUPPLEMENTAL INFORMATION

Supplemental Information can be found online at https://doi.org/10.1016/j.omtn.2019.09.006.

AUTHOR CONTRIBUTIONS

Y.L., S.Z., and W.P. conceived and designed the study. Y.L., S.Z., C.H., P.J., L.Z., Y.Z., and Z.L. performed the experiments. Y.L., S.Z., X.X., and W.P. analyzed the data. Y.L., S.Z., and W.P. wrote the manuscript. All authors read and approved the final manuscript.

CONFLICTS OF INTEREST

The authors declare no competing interests.

ACKNOWLEDGMENTS

We thank the staff of the National Institute of Parasitic Disease, Chinese Center for Disease Control and Prevention for their help with

parasite infections. This study was supported by the National Natural Science Foundation of China (81430051).

REFERENCES

1. Bartel, D.P. (2004). MicroRNAs: genomics, biogenesis, mechanism, and function. Cell *116*, 281–297.
2. Calin, G.A., and Croce, C.M. (2006). MicroRNA signatures in human cancers. Nat. Rev. Cancer *6*, 857–866.
3. Berindan-Neagoe, I., Monroig, Pdel.C., Pasculli, B., and Calin, G.A. (2014). MicroRNAome genome: a treasure for cancer diagnosis and therapy. CA Cancer J. Clin. *64*, 311–336.
4. Mi, Y., Zhang, D., Jiang, W., Weng, J., Zhou, C., Huang, K., Tang, H., Yu, Y., Liu, X., Cui, W., et al. (2017). miR-181a-5p promotes the progression of gastric cancer via RASSF6-mediated MAPK signalling activation. Cancer Lett. *389*, 11–22.
5. Zhu, Y., Gu, J., Li, Y., Peng, C., Shi, M., Wang, X., Wei, G., Ge, O., Wang, D., Zhang, B., et al. (2018). miR-17-5p enhances pancreatic cancer proliferation by altering cell cycle profiles via disruption of RBL2/E2F4-repressing complexes. Cancer Lett. *412*, 59–68.
6. Fang, Y., Xue, J.L., Shen, Q., Chen, J., and Tian, L. (2012). MicroRNA-7 inhibits tumor growth and metastasis by targeting the phosphoinositide 3-kinase/Akt pathway in hepatocellular carcinoma. Hepatology *55*, 1852–1862.
7. Hatziapostolou, M., Polytarchou, C., Aggelidou, E., Drakaki, A., Poultsides, G.A., Jaeger, S.A., Ogata, H., Karin, M., Struhl, K., Hadzopoulou-Cladaras, M., and Iliopoulos, D. (2011). An HNF4α-miRNA inflammatory feedback circuit regulates hepatocellular oncogenesis. Cell *147*, 1233–1247.
8. Théry, C. (2011). Exosomes: secreted vesicles and intercellular communications. F1000 Biol. Rep. *3*, 15.
9. Chin, A.R., Fong, M.Y., Somlo, G., Wu, J., Swiderski, P., Wu, X., and Wang, S.E. (2016). Cross-kingdom inhibition of breast cancer growth by plant miR159. Cell Res. *26*, 217–228.
10. Zhang, L., Hou, D., Chen, X., Li, D., Zhu, L., Zhang, Y., Li, J., Bian, Z., Liang, X., Cai, X., et al. (2012). Exogenous plant MIR168a specifically targets mammalian LDLRAP1: evidence of cross-kingdom regulation by microRNA. Cell Res. *22*, 107–126.
11. Zhou, Z., Li, X., Liu, J., Dong, L., Chen, Q., Liu, J., Kong, H., Zhang, Q., Qi, X., Hou, D., et al. (2015). Honeysuckle-encoded atypical microRNA2911 directly targets influenza A viruses. Cell Res. *25*, 39–49.
12. Buck, A.H., Coakley, G., Simbari, F., McSorley, H.J., Quintana, J.F., Le Bihan, T., Kumar, S., Abreu-Goodger, C., Lear, M., Harcus, Y., et al. (2014). Exosomes secreted by nematode parasites transfer small RNAs to mammalian cells and modulate innate immunity. Nat. Commun. *5*, 5488.
13. Stern-Ginossar, N., Elefant, N., Zimmermann, A., Wolf, D.G., Saleh, N., Biton, M., Horwitz, E., Prokocimer, Z., Prichard, M., Hahn, G., et al. (2007). Host immune system gene targeting by a viral miRNA. Science *317*, 376–381.
14. Liu, H., Wang, X., Wang, H.D., Wu, J., Ren, J., Meng, L., Wu, Q., Dong, H., Wu, J., Kao, T.Y., et al. (2012). *Escherichia coli* noncoding RNAs can affect gene expression and physiology of *Caenorhabditis elegans*. Nat. Commun. *3*, 1073.
15. Wang, Z., Xue, X., Sun, J., Luo, R., Xu, X., Jiang, Y., Zhang, Q., and Pan, W. (2010). An "in-depth" description of the small non-coding RNA population of *Schistosoma japonicum* schistosomulum. PLoS Negl. Trop. Dis. *4*, e596.
16. Xue, X., Sun, J., Zhang, Q., Wang, Z., Huang, Y., and Pan, W. (2008). Identification and characterization of novel microRNAs from *Schistosoma japonicum*. PLoS ONE *3*, e4034.
17. Zhu, S., Wang, S., Lin, Y., Jiang, P., Cui, X., Wang, X., Zhang, Y., and Pan, W. (2016). Release of extracellular vesicles containing small RNAs from the eggs of *Schistosoma japonicum*. Parasit. Vectors *9*, 574.
18. Cheng, G., Luo, R., Hu, C., Cao, J., and Jin, Y. (2013). Deep sequencing-based identification of pathogen-specific microRNAs in the plasma of rabbits infected with *Schistosoma japonicum*. Parasitology *140*, 1751–1761.
19. Hao, L., Cai, P., Jiang, N., Wang, H., and Chen, Q. (2010). Identification and characterization of microRNAs and endogenous siRNAs in *Schistosoma japonicum*. BMC Genomics *11*, 55.
20. Hou, J., Lin, L., Zhou, W., Wang, Z., Ding, G., Dong, Q., Qin, L., Wu, X., Zheng, Y., Yang, Y., et al. (2011). Identification of miRNomes in human liver and hepatocellular carcinoma reveals miR-199a/b-3p as therapeutic target for hepatocellular carcinoma. Cancer Cell *19*, 232–243.
21. Chen, L., Zheng, J., Zhang, Y., Yang, L., Wang, J., Ni, J., Cui, D., Yu, C., and Cai, Z. (2011). Tumor-specific expression of microRNA-26a suppresses human hepatocellular carcinoma growth via cyclin-dependent and -independent pathways. Mol. Ther. *19*, 1521–1528.
22. Huang, J., Hao, P., Chen, H., Hu, W., Yan, Q., Liu, F., and Han, Z.G. (2009). Genome-wide identification of *Schistosoma japonicum* microRNAs using a deep-sequencing approach. PLoS ONE *4*, e8206.
23. Mountford, J.K., Petitjean, C., Putra, H.W., McCafferty, J.A., Setiabakti, N.M., Lee, H., Tønnesen, L.L., McFadyen, J.D., Schoenwaelder, S.M., Eckly, A., et al. (2015). The class II PI 3-kinase, PI3KC2α, links platelet internal membrane structure to shear-dependent adhesive function. Nat. Commun. *6*, 6535.
24. Yoshioka, K., Yoshida, K., Cui, H., Wakayama, T., Takuwa, N., Okamoto, Y., Du, W., Qi, X., Asanuma, K., Sugihara, K., et al. (2012). Endothelial PI3K-C2α, a class II PI3K, has an essential role in angiogenesis and vascular barrier function. Nat. Med. *18*, 1560–1569.
25. IARC Working Group on the Evaluation of Carcinogenic Risks to Humans (2007). Human papillomaviruses. IARC Monogr. Eval. Carcinog. Risks Hum. *90*, 1–636.
26. Blumberg, B.S., Larouzé, B., London, W.T., Werner, B., Hesser, J.E., Millman, I., Saimot, G., and Payet, M. (1975). The relation of infection with the hepatitis B agent to primary hepatic carcinoma. Am. J. Pathol. *81*, 669–682.
27. IARC working group on the evaluation of carcinogenic risks to humans (1994). some industrial chemicals. Lyon, 15–22 February 1994. IARC Monogr. Eval. Carcinog. Risks Hum. *60*, 1–560.
28. Bouvard, V., Baan, R., Straif, K., Grosse, Y., Secretan, B., El Ghissassi, F., Benbrahim-Tallaa, L., Guha, N., Freeman, C., Galichet, L., and Cogliano, V.; WHO International Agency for Research on Cancer Monograph Working Group (2009). A review of human carcinogens—Part B: biological agents. Lancet Oncol. *10*, 321–322.
29. IARC Working Group on the Evaluation of Carcinogenic Risks to Humans (2012). Biological agents. Volume 100B. A review of human carcinogens. IARC Monogr. Eval. Carcinog. Risks Hum. *100*, 1–441.
30. Gryseels, B., Polman, K., Clerinx, J., and Kestens, L. (2006). Human schistosomiasis. Lancet *368*, 1106–1118.
31. Liu, B.Q., Rong, Z.P., Sun, X.T., Wu, Y.P., and Gao, R.Q. (1983). [Geographical correlation between colorectal cancer and schistosomiasis in China]. Zhongguo Yi Xue Ke Xue Yuan Xue Bao *5*, 173–177.
32. Guo, Z.R., Ni, Yc., and Wu, J.L. (1984). Epidemiological study on relationship between schistosomiasis and colorectal cancer. Jiangsu Med. J. *4*, 209.
33. Arzumanyan, A., Reis, H.M., and Feitelson, M.A. (2013). Pathogenic mechanisms in HBV- and HCV-associated hepatocellular carcinoma. Nat. Rev. Cancer *13*, 123–135.
34. Coussens, L.M., and Werb, Z. (2002). Inflammation and cancer. Nature *420*, 860–867.
35. Kundu, J.K., and Surh, Y.J. (2008). Inflammation: gearing the journey to cancer. Mutat. Res. *659*, 15–30.
36. Ohshima, H., and Bartsch, H. (1994). Chronic infections and inflammatory processes as cancer risk factors: possible role of nitric oxide in carcinogenesis. Mutat. Res. *305*, 253–264.
37. Takemura, Y., Kikuchi, S., and Inaba, Y. (1998). Epidemiologic study of the relationship between schistosomiasis due to Schistosoma japonicum and liver cancer/cirrhosis. Am. J. Trop. Med. Hyg. *59*, 551–556.
38. Zhang, R., Takahashi, S., Orita, S., Yoshida, A., Maruyama, H., Shirai, T., and Ohta, N. (1998). *p*53 Gene mutations in rectal cancer associated with schistosomiasis japonica in Chinese patients. Cancer Lett. *131*, 215–221.
39. Honeycutt, J., Hammam, O., Fu, C.L., and Hsieh, M.H. (2014). Controversies and challenges in research on urogenital schistosomiasis-associated bladder cancer. Trends Parasitol. *30*, 324–332.

40. van Tong, H., Brindley, P.J., Meyer, C.G., and Velavan, T.P. (2017). Parasite infection, carcinogenesis and human malignancy. EBioMedicine *15*, 12–23.

41. Islam, W., Islam, S.U., Qasim, M., and Wang, L. (2017). Host-pathogen interactions modulated by small RNAs. RNA Biol. *14*, 891–904.

42. Knip, M., Constantin, M.E., and Thordal-Christensen, H. (2014). Trans-kingdom cross-talk: small RNAs on the move. PLoS Genet. *10*, e1004602.

43. Lee, Y., Ahn, C., Han, J., Choi, H., Kim, J., Yim, J., Lee, J., Provost, P., Rådmark, O., Kim, S., and Kim, V.N. (2003). The nuclear RNase III Drosha initiates microRNA processing. Nature *425*, 415–419.

44. Sperber, H., Beem, A., Shannon, S., Jones, R., Banik, P., Chen, Y., Ku, S., Varani, G., Yao, S., and Ruohola-Baker, H. (2014). miRNA sensitivity to Drosha levels correlates with pre-miRNA secondary structure. RNA *20*, 621–631.

45. Zhou, Y., Geng, P., Liu, Y., Wu, J., Qiao, H., Xie, Y., Yin, N., Chen, L., Lin, X., Liu, Y., et al. (2018). Rotavirus-encoded virus-like small RNA triggers autophagy by targeting IGF1R via the PI3K/Akt/mTOR pathway. Biochim. Biophys. Acta Mol. Basis Dis. *1864*, 60–68.

46. Ng, S.K., Neo, S.Y., Yap, Y.W., Karuturi, R.K., Loh, E.S., Liau, K.H., and Ren, E.C. (2009). Ablation of phosphoinositide-3-kinase class II alpha suppresses hepatoma cell proliferation. Biochem. Biophys. Res. Commun. *387*, 310–315.

47. Yoon, S., Han, E., Choi, Y.C., Kee, H., Jeong, Y., Yoon, J., and Baek, K. (2014). Inhibition of cell proliferation and migration by miR-509-3p that targets CDK2, Rac1, and PIK3C2A. Mol. Cells *37*, 314–321.

48. Chao, L.M., Sun, W., Chen, H., Liu, B.Y., Li, P.F., and Zhao, D.W. (2018). MicroRNA-31 inhibits osteosarcoma cell proliferation, migration and invasion by targeting PIK3C2A. Eur. Rev. Med. Pharmacol. Sci. *22*, 7205–7213.

49. Skeen, J.E., Bhaskar, P.T., Chen, C.C., Chen, W.S., Peng, X.D., Nogueira, V., Hahn-Windgassen, A., Kiyokawa, H., and Hay, N. (2006). Akt deficiency impairs normal cell proliferation and suppresses oncogenesis in a p53-independent and mTORC1-dependent manner. Cancer Cell *10*, 269–280.

50. Dennis, P.B., Jaeschke, A., Saitoh, M., Fowler, B., Kozma, S.C., and Thomas, G. (2001). Mammalian TOR: a homeostatic ATP sensor. Science *294*, 1102–1105.

51. Yuan, H.X., and Guan, K.L. (2016). Structural insights of mTOR complex 1. Cell Res. *26*, 267–268.

52. Gulhati, P., Bowen, K.A., Liu, J., Stevens, P.D., Rychahou, P.G., Chen, M., Lee, E.Y., Weiss, H.L., O'Connor, K.L., Gao, T., and Evers, B.M. (2011). mTORC1 and mTORC2 regulate EMT, motility, and metastasis of colorectal cancer via RhoA and Rac1 signaling pathways. Cancer Res. *71*, 3246–3256.

53. Wang, Y., Wang, Q., Gao, L., Zhu, B., Ju, Z., Luo, Y., and Zuo, J. (2017). Parsing the regulatory network between small RNAs and target genes in ethylene pathway in tomato. Front. Plant Sci. *8*, 527.

54. Zhao, L., Lu, H., Meng, Q., Wang, J., Wang, W., Yang, L., and Lin, L. (2016). Profilings of microRNAs in the liver of common carp (*Cyprinus carpio*) infected with *Flavobacterium columnare*. Int. J. Mol. Sci. *17*, 566.

55. Li, R., Zhang, C.L., Liao, X.X., Chen, D., Wang, W.Q., Zhu, Y.H., Geng, X.H., Ji, D.J., Mao, Y.J., Gong, Y.C., and Yang, Z.P. (2015). Transcriptome microRNA profiling of bovine mammary glands infected with *Staphylococcus aureus*. Int. J. Mol. Sci. *16*, 4997–5013.

56. Cai, P., Piao, X., Hao, L., Liu, S., Hou, N., Wang, H., and Chen, Q. (2013). A deep analysis of the small non-coding RNA population in *Schistosoma japonicum* eggs. PLoS ONE *8*, e64003.

57. He, X., Xie, J., Zhang, D., Su, Q., Sai, X., Bai, R., Chen, C., Luo, X., Gao, G., and Pan, W. (2015). Recombinant adeno-associated virus-mediated inhibition of microRNA-21 protects mice against the lethal schistosome infection by repressing both IL-13 and transforming growth factor beta 1 pathways. Hepatology *61*, 2008–2017.

58. Zhu, L., Liu, J., Dao, J., Lu, K., Li, H., Gu, H., Liu, J., Feng, X., and Cheng, G. (2016). Molecular characterization of *S. japonicum* exosome-like vesicles reveals their regulatory roles in parasite-host interactions. Sci. Rep. *6*, 25885.

59. Yin, X., Xiang, T., Li, L., Su, X., Shu, X., Luo, X., Huang, J., Yuan, Y., Peng, W., Oberst, M., et al. (2013). *DACT1*, an antagonist to Wnt/β-catenin signaling, suppresses tumor cell growth and is frequently silenced in breast cancer. Breast Cancer Res. *15*, R23.